Umklapp surface reflection of conduction electrons*

Richard M. More
Department of Physics, University of Pittsburgh, Pittsburgh, Pennsylvania 15260
(Received 23 July 1973)

The specular reflection of conduction electrons is limited, even at an ideal metal surface, by a mechanism suggested by Price. This process, loosely called umklapp surface scattering, is studied theoretically in this paper. The grazing-incidence behavior is analyzed, and special singularities in the reflection coefficients are predicted. The singularities are related in a simple manner to the Fermi-surface geometry. The results appear relevant to experiments on magnetic surface-state resonance, the anomalous skin effect, and the thin-film size effect. The umklapp mechanism is interesting especially because it represents an *intrinsic* limit on specular reflection which cannot be removed by cleaning and polishing the specimen.

I. INTRODUCTION

New experimental techniques, such as magnetic surface-state resonance,[1] have revived theoretical interest in the diffuse and specular reflection of conduction electrons at metal surfaces. For specially prepared surfaces of Ga, In, Sb, Bi, Zn, and even Cu, surface-state-resonance experiments show that a large fraction of electrons are specularly reflected (at grazing incidence).[1-3] Such specular reflection is obviously limited by surface roughness[4,5] and by adsorbed contaminant or oxide layers,[6,7] but the specular reflection is also limited by an intrinsic mechanism that applies even at an ideal metal surface.

This additional mechanism is one in which an electron jumps to a distant point on the Fermi surface during reflection (while still conserving the component of its wave vector parallel to the crystal surface). The process may be loosely described as umklapp surface scattering.[8] Originally suggested by Price,[9] the effect was briefly discussed by Pippard,[10] Chambers,[11] Greene,[12] and Friedman,[13] but apparently has never been studied in detail. The umklapp mechanism is interesting especially because it represents an *intrinsic* limitation on specular reflection which cannot be removed by cleaning or polishing the specimen.

This paper constructs a theory for umklapp surface scattering in a simple situation of high symmetry. We show that the reflection becomes specular at grazing incidence, determine the power law of this angle dependence, and predict where on the Fermi surface the umklapp mechanism is most likely to be observed. For certain crystal orientations, our theory predicts that the reflection probability will show characteristic singularities related to extremal points of the band structure.

The umklapp surface scattering is most likely to be unambiguously detected by surface-state-resonance experiments, for those experiments focus on electrons of the metal with definite angles of incidence. But the umklapp scattering may also prove to play an important role in thin-film resistivity (size effect) or even quantum-limit behavior in thin films, as well as for the anomalous skin effect or other surface-related topics of traditional metal physics.

To illustrate a specific case, a section of the Cu Fermi surface is shown in Fig. 1. If a conduction electron at point A on this diagram approaches the metal surface, the usual specular reflection transfers it to the nearby image point A′. During this transition, the component $\vec{K}_{\parallel}$ of wave vector parallel to the crystal surface is conserved. The electron velocity in state A′ is the reflection of the original velocity in the surface plane; but the electron can also jump from A to the distant point B on the neck of the Fermi surface (again conserving $\vec{K}_{\parallel}$). The velocity at B also points back into the bulk, but has changed magnitude and direction and the reflection from A to B is nonspecular. (Although nonspecular, it is not diffuse.) Because of the anisotropic distribution of necks on the Cu Fermi surface, electron surface reflection near point A should be anisotropic with respect to the plane of incidence. Experimental search for this anisotropy is feasible with existing surface-state-resonance techniques.[1-4]

Section II sets up a mathematical description of the jump-scattering process for an idealized Fermi surface. General properties of the reflection coefficients are identified by adaptation of nuclear-reaction scattering theory. The small-angle (grazing-incidence) behavior is determined by a special negative-angle symmetry.[6] The grazing-incidence expansion, and a related discussion of singular points, is given in Sec. III. Since the grazing-incidence scattering involves extremal points on the Fermi surface, it is not surprising that the angle dependences exhibit a characteristic structure determined only by the Fermi-surface geometry.

In Sec. IV the probability of specular reflection is formally calculated in terms of Bloch functions

and a surface boundary condition. The results illustrate and verify the symmetry discussion of Secs. II and III. It is noted that for a special (unrealistic) boundary condition, $\Psi = 0$ at the surface, there is *no* umklapp surface scattering.

Stern and Howard,[14] in a discussion of semiconductor inversion layers, adopted this boundary condition ($\Psi = 0$) to avoid *intervalley* surface scattering. In fact, intervalley surface scattering is an instance of the mechanism considered in this paper, although in the semiconductor case the term "umklapp" becomes especially inappropriate.[8] Kravchenko and Rashba[15] have recently considered the carrier redistribution among valleys in the presence of intervalley scattering, but they directed their attention primarily toward electrostatic effects which do not arise in metals.

Section V concludes our discussion and mentions some applications. The Appendix is devoted to a wave-packet analysis of the *definition* of reflection probability. Although this definition is plausible, it requires careful discussion because it plays a basic role in the theory.

II. SURFACE-REFLECTION MATRIX

The analysis to follow is limited to low-index surfaces which have the full translational periodicity (parallel to the surface) of the bulk metal. We shall neglect surface roughness and contamination effects. If the surface has this translational symmetry, then the parallel component of the electron wave vector is conserved during collision with the surface, along with the electron energy.[9,16] The wave vector of the electron changes during reflection to one of the points of intersection of the Fermi surface with the *line* of constant $\vec{K}_{\parallel}$.

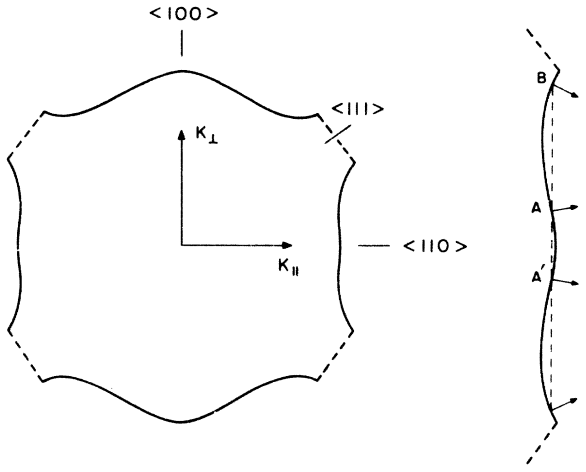

FIG. 1. Cross section of the Cu Fermi surface, to illustrate the umklapp scattering process. The crystal is cut so that the ⟨100⟩ wave vector ($\vec{K}_\perp$) is normal to the surface. Electron states near point A are approaching the crystal surface from below. Reflection from A to A′ is the usual specular reflection. Reflection from A to the neck state B is the jump scattering or "umklapp" process. In preparing this drawing, the Cu Fermi surface was *assumed* to be convex near point A.

For convenience, our discussion is phrased in terms of an idealized Fermi surface, shown in Fig. 2. While very simple, this Fermi surface still exhibits the most interesting effects; however the discussion is easily adapted to more lifelike geometries.[17] For the value of $\vec{K}_{\parallel}$ shown in Fig. 2, there are four relevant Bloch states; ϕ_1 and ϕ_2 are Bloch waves approaching the crystal surface and $\tilde{\phi}_1$ and $\tilde{\phi}_2$ are Bloch waves leaving the surface (the electron velocity is the local normal to the Fermi surface).

Two independent scattering solutions of the complete Schrödinger equation exist in this case and these are *uniquely* specified by their incident wave parts[18]:

$$\Psi_i = \phi_i + \sum_k R_{ik}\tilde{\phi}_k + \Psi_i^{\mathrm{loc}}, \quad i = 1, 2 \text{ and } k = 1, 2 \quad . \tag{1}$$

R_{ik} is a reflection coefficient which indicates the amplitude of the reflected wave $\tilde{\phi}_k$; R_{ik} is a function of $\vec{K}_{\parallel}$ and would also depend on energy if that were not fixed at the Fermi level. In general the wave function Ψ_i contains a part localized near the surface, denoted Ψ_i^{loc}, which decays with distance into the bulk. Our attention will focus on the region *far* from the surface, i.e., on the asymptotic form of the wave function, which contains only propagating waves:

$$\Psi_1 = \phi_1 + R_{11}\tilde{\phi}_1 + R_{12}\tilde{\phi}_2 \quad , \tag{2}$$

$$\Psi_2 = \phi_2 + R_{21}\tilde{\phi}_1 + R_{22}\tilde{\phi}_2 \quad . \tag{2'}$$

The functions $\phi_j(\vec{r})$ are Bloch functions of the infinite crystal and have the usual form in the region far from the surface:

$$\phi_j(\vec{r}) = u_j(\vec{r})\, e^{i\vec{K}_j\cdot\vec{r}} \quad . \tag{3}$$

Changes in the Bloch functions near the crystal surface may be thought to be included in the localized term Ψ_i^{loc} of Eq. (1) and need not be considered in the asymptotic region. It is convenient to fix the normalization of the Bloch functions so that $\phi_j(\vec{r})$ is normalized to a constant on the unit cell and the constant may be chosen to be unity:

$$\int |\phi_i(\vec{r})|^2 d^3r = 1 \quad . \tag{3'}$$

The wave functions Ψ_i are scattering solutions of the time-independent Schrödinger equation, but it is useful to keep in mind their wave-packet interpretation. If an appropriate superposition is made of states near Ψ_1, for example, then one has a state which begins as a wave packet of type ϕ_1 *approaching* the crystal surface, and later is a

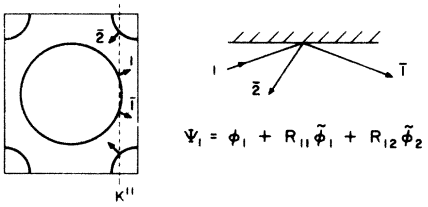

FIG. 2. Model Fermi surface chosen to illustrate the umklapp surface scattering. The Fermi surface consists of a central electron sphere and also a set of smaller electron spherical pockets at the corners of the zone. A representative value of $\vec{K}_{II}$ is shown. The inset on the right shows the wave function Ψ_1 for this case.

superposition of reflected wave packets of types $\tilde{\phi}_1$ and $\tilde{\phi}_2$ leaving the surface. Since these two reflected wave packets have different velocities, they will separate from each other and there will be no interference between them in the reflected current or reflection probability.

With this wave-packet interpretation in mind, we define the probability of reflection from incident state ϕ_i to reflected state $\tilde{\phi}_k$ as the *ratio* of normal components of the reflected current density of state k to the incident current density in state i:

$$P_{ik} \equiv \vec{\hat{n}} \cdot \vec{J}_k / \vec{\hat{n}} \cdot \vec{J}_i \quad . \tag{4}$$

The currents are computed from the asymptotic wave function of Eq. (2); $\vec{\hat{n}}$ is a unit vector normal to the crystal surface. The projection of the currents onto the normal is very natural because electron motion along the surface does not by itself constitute collision with the surface. The definition of Eq. (4) is an important part of the work of this section and is further clarified by a wave-packet discussion given in the Appendix. It is shown there that P_{ik} is the total probability in the reflected wave packet of type k for a normalized incident wave packet of type i.

If $\vec{v}_i$ is the electron velocity at a point i on the Fermi surface, the probability P_{ik} computed from Eq. (2) is

$$P_{ik} = \frac{\vec{\hat{n}} \cdot \vec{v}_k}{\vec{\hat{n}} \cdot \vec{v}_i} |R_{ik}|^2 \quad , \tag{4'}$$

where again $\vec{\hat{n}}$ is the unit normal to the surface. We introduce angles of incidence of the beams measured between the *velocity* vector and the surface *plane*; θ is the angle of incidence of beam 1 and ϕ is the angle of incidence of beam 2 (see Fig. 3). In terms of these angles, Eq. (4′) reads

$$P_{11} = |R_{11}|^2 \quad ,$$

$$P_{12} = \frac{v_2 \sin\phi}{v_1 \sin\theta} |R_{12}|^2 \quad , \tag{5}$$

$$P_{21} = \frac{v_1 \sin\theta}{v_2 \sin\phi} |R_{21}|^2 \quad ,$$

$$P_{22} = |R_{22}|^2 \quad .$$

For a smooth-metal surface, with no diffuse scattering, an incident electron must appear in states $\tilde{\phi}_1$ and $\tilde{\phi}_2$ and nowhere else. This implies that probability is conserved in the sense that

$$\sum_{k=1}^{2} P_{ik} = 1 \quad (i = 1, 2)$$

or, explicitly,

$$|R_{11}|^2 + \frac{v_2 \sin\phi}{v_1 \sin\theta} |R_{12}|^2 = 1 \quad , \tag{6a}$$

$$|R_{22}|^2 + \frac{v_1 \sin\theta}{v_2 \sin\phi} |R_{21}|^2 = 1 \quad . \tag{6b}$$

There is an additional equation implied by probability conservation, however, and that is

$$\frac{R_{21}}{R_{22}} + \frac{v_2 \sin\phi}{v_1 \sin\theta} \left(\frac{R_{12}}{R_{11}}\right)^* = 0 \quad . \tag{6c}$$

Equation (6c) is required in order that probability be conserved not only for the incident waves ϕ_1 and ϕ_2 but also for any linear combination of the two.

Another general limitation is imposed on R_{ik} by time-reversal symmetry:

$$\sum_j R_{ij}^* R_{jk} = \delta_{ik} \quad . \tag{7}$$

This equation, like that for the conservation of probability, applies in the form given only to reflection from a smooth surface. In this case the electron wave equation is invariant under time reversal, which reverses the velocities of electrons. Let it be further assumed that the surface has 180° rotation symmetry about the unit normal $\vec{\hat{n}}$.[17] Under the combined symmetry T of time reversal and 180° rotation, the incident and reflected Bloch waves are simply interchanged:

$$T\phi_i = \tilde{\phi}_i; \quad T\tilde{\phi}_i = \phi_i \quad (i = 1, 2) \quad .$$

If the electron Hamiltonian has time reversal and rotation symmetry T, then $T\Psi_1$ is also a solution

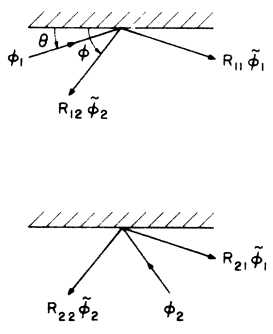

FIG. 3. (a) Surface scattering state $\Psi_1 = \phi_1 + R_{11}\tilde{\phi}_1 + R_{12}\tilde{\phi}_2$, with angles θ, ϕ identified. (b) Surface scattering state $\Psi_2 = \phi_2 + R_{21}\tilde{\phi}_1 + R_{22}\tilde{\phi}_2$.

of the Schrödinger equation and so must be some linear combination of Ψ_1 and Ψ_2. It is possible to exhibit this linear combination if one recalls that time reversal has the effect of complex-conjugating the expansion coefficients in a superposition:

$$T\Psi_1 = T\phi_1 + R_{11}^* T\tilde{\phi}_1 + R_{12}^* T\tilde{\phi}_2$$
$$= \tilde{\phi}_1 + R_{11}^* \phi_1 + R_{12}^* \phi_2 \quad .$$

The incident wave part of this expression is $R_{11}^* \phi_1 + R_{12}^* \phi_2$, which uniquely determines the coefficients in the expansion of $T\Psi_1$ as a superposition of Ψ_1 and Ψ_2:

$$T\Psi_1 = R_{11}^* \Psi_1 + R_{12}^* \Psi_2 \quad .$$

A similar equation holds for $T\Psi_2$:

$$T\Psi_2 = \tilde{\phi}_2 + R_{21}^* \phi_1 + R_{22}^* \phi_2 = R_{21}^* \Psi_1 + R_{22}^* \Psi_2 \quad .$$

Equation (7) follows from these two equations when coefficients of the waves $\tilde{\phi}_j$ are equated. A more extensive discussion of time reversal and probability conservation is given by Blatt and Weisskopf for the analogous case of nuclear-reaction scattering.[19]

A useful formula is deduced by combining Eqs. (6) and (7):

$$\frac{R_{12}}{R_{21}} = \frac{v_1 \sin\theta}{v_2 \sin\phi} \quad . \tag{8}$$

If Eq. (8) is substituted into Eq. (5), one finds the expected connection between the probabilities of the reciprocal transitions $1 \to 2$ and $2 \to 1$,

$$P_{12} = P_{21} \quad . \tag{9}$$

This equation follows from probability conservation and time reversal in the forms (6) and (7), respectively. Equation (9) expresses the principle of *detailed balance* and is a requirement for thermal equilibrium between electrons at different points on the Fermi surface.[20]

Another symmetry, quite distinct from time-reversal symmetry, plays a useful role in predicting the glancing incidence behavior. This additional symmetry refers to the extension of the reflection coefficients to *negative angles of incidence*.[6] The argument given in this section is quite abstract and the reader will find it useful to examine both the explicit form of R_{ik} constructed in Sec. IV and also general works on collision theory (where a similar symmetry property appears in the form of the Jost function representation of the scattering amplitude or S matrix).[21] The effective result of the discussion to follow is the set of Eqs. (12), which are applied in Sec. III.

The wave function $\Psi_1 \equiv \Psi_\theta^{(1)}$, considered now as a mathematical function of the angle of incidence θ, may be continued to negative values of that angle. The analytic continuation is never difficult when an explicit formula for $R_{ik}(\theta)$ is available. The negative-angle wave-function does *not* refer to electrons incident from the vacuum outside the metal; indeed the electrons are confined to the metal at the energy considered ($E = E_F$) for any angle θ. Rather, $\Psi_{-\theta}^{(1)}$ obeys a special boundary condition which may be understood by following the changes in $\Psi_\theta^{(1)}$ as θ is decreased through zero.

The analytic continuation $\Psi_{-\theta}^{(1)}$ is depicted in Fig. 4 (θ is a positive number). This wave function consists of a beam $\tilde{\phi}_1$ of unit strength leaving the surface (this term is the analytic continuation of the original incident beam), a beam ϕ_1 of strength $R_{11}(-\theta)$ approaching the surface (this is the continuation of the original reflected beam $R_{11}\tilde{\phi}_1$) and a second reflected beam $\tilde{\phi}_2$ of strength $R_{12}(-\theta)$. In the continued wave function $\Psi_{-\theta}^{(1)}$, then, beams ϕ_1 and ϕ_1 have interchanged roles with no change in ϕ_2 (the latter point is amplified below). The coefficients $R_{11}(-\theta)$ and $R_{12}(-\theta)$ are obtained by analytic continuation, but they are *also* the values such that $\Psi_{-\theta}^{(1)}$ solves the Schrödinger equation.

Thus the continuation of Ψ_1 to negative angles of incidence has the form

$$\Psi_{-\theta}^{(1)} = \tilde{\phi}_1 + R_{11}(-\theta)\phi_1 + R_{12}(-\theta)\tilde{\phi}_2 \quad . \tag{10}$$

The incident wave part of this expression is $R_{11}(-\theta)\phi_1$ and because the scattering state is uniquely specified by its incident wave part, the state $\Psi_{-\theta}^{(1)}$ must equal $R_{11}(-\theta)\Psi_\theta^{(1)}$.

In the same way the scattering state $\Psi_\theta^{(2)} \equiv \Psi_2$, when continued to angle $-\theta$, becomes

$$\Psi_{-\theta}^{(2)} = \phi_2 + R_{21}(-\theta)\phi_1 + R_{22}(-\theta)\tilde{\phi}_2 \quad . \tag{10'}$$

The incident wave part of this is $\phi_2 + R_{21}(-\theta)\phi_1$ and so this must equal $\Psi_\theta^{(2)} + R_{21}(-\theta)\Psi_\theta^{(1)}$. To summarize, the continued wave functions are

$$\Psi_{-\theta}^{(1)} = R_{11}(-\theta)\Psi_\theta^{(1)} \quad ,$$
$$\Psi_{-\theta}^{(2)} = \Psi_\theta^{(2)} + R_{21}(-\theta)\Psi_\theta^{(1)} \quad . \tag{11}$$

Equations (10) and (11) are easily translated into conditions on the reflection matrix $R_{ik}(-\theta)$ by comparing coefficients of the reflected waves $\tilde{\phi}_k$. The resulting equations are

$$R_{11}(-\theta) = 1/R_{11}(\theta) \quad , \tag{12a}$$

$$R_{12}(-\theta) = R_{12}(\theta)/R_{11}(\theta) \quad , \tag{12b}$$

$$R_{21}(-\theta) = -R_{21}(\theta)/R_{11}(\theta) \quad , \tag{12c}$$

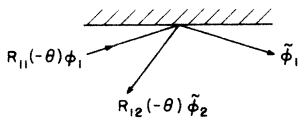

FIG. 4. State $\Psi_{-\theta}^{(1)}$ corresponding to a negative angle of incidence for state ϕ_1.

$$R_{22}(-\theta) = R_{22}(\theta) - R_{12}(\theta)R_{21}(\theta)/R_{11}(\theta) \quad . \qquad (12d)$$

This set of equations follows from the assertion that the analytic continuation wave functions $\Psi^{(j)}_{-\theta}$ are solutions of the original Schrödinger equation. It is quite possible that this symmetry breaks down in the presence of important spin-orbit coupling or other velocity dependence of the potential. In Sec. IV the wave equation is solved with a fixed (velocity-independent) boundary condition imposed at the metal surface, and the resulting closed-form expressions for R_{ik} obey the symmetry given in Eqs. (12).

To further clarify the meaning of Eqs. (12), we note that the reflection matrix is a function of the electron energy (fixed at the Fermi energy) and of the parallel wave vector $\vec{K}_{\parallel}$. R_{ik} is not a single-valued function of $\vec{K}_{\parallel}$ because each fixed value of $\vec{K}_{\parallel}$ is compatible with positive or negative angles of incidence. The change from positive to negative angle θ is simply an exchange of *labels* of beams ϕ_1 and $\bar{\phi}_1$ (while ϕ_2 and $\bar{\phi}_2$ are unaltered). R_{ik} has a branch-cut (as a function of $\vec{K}_{\parallel}$) joining the extremal points where beam ϕ_1 is at grazing incidence. The values of R_{ik} on the two sides of this branch-cut are then linked by Eqs. (12); the usual side of the branch-cut, on which $\theta > 0$, corresponds to the usual scattering boundary conditions of Fig. 3.

An entirely analogous analytic structure is associated with the angle ϕ, i.e., with the analytic continuation of R_{ik} which exchanges labels of beams ϕ_2 and $\bar{\phi}_2$ without affecting beam ϕ_1. This symmetry may be analyzed in the same way and gives rise to Eqs. (13):

$$R_{11}(-\phi) = R_{11}(\phi) - R_{12}(\phi)R_{21}(\phi)/R_{22}(\phi) \quad , \qquad (13a)$$

$$R_{12}(-\phi) = -R_{12}(\phi)/R_{22}(\phi) \quad , \qquad (13b)$$

$$R_{21}(-\phi) = R_{21}(\phi)/R_{22}(\phi) \quad , \qquad (13c)$$

$$R_{22}(-\phi) = 1/R_{22}(\phi) \quad . \qquad (13d)$$

It is also possible to simultaneously exchange θ with $-\theta$ and ϕ with $-\phi$. This complete symmetry inverts the matrix of reflection coefficients, as may be verified by an analysis like that given in Eqs. (10) and (11):

$$[R(-\theta, -\phi)]_{ik} = [R^{-1}(\theta, \phi)]_{ik} \quad . \qquad (14)$$

As shown in Sec III, Eqs. (12)–(14) limit the small-angle scattering in a powerful way. The symmetries do not make possible a numerical calculation of the reflection matrix (information about the surface potential is required for that) but they do yield restrictions on R_{ik} which greatly reduce the number of free parameters. The resulting expansion is similar to the effective-range expansion for nuclear-reaction threshhold scattering, but is applied here not to the energy dependence but rather to the *angle dependence* of the reflection amplitudes.

III. GRAZING-INCIDENCE BEHAVIOR

For magnetic surface state resonance, or for the anomalous skin effect, the electrons of greatest interest are those which approach the metal surface at glancing or grazing incidence. It is desirable to determine the general nature of grazing-incidence scattering, and fortunately that case is primarily governed by simple geometric features of the band structure. This means that the results to follow are easily adapted to any metal.

Two general statements will be shown to describe the umklapp surface reflection: First, the surface reflection becomes specular at grazing incidence according to the linear law

$$P(\theta) = 1 - 2\alpha\theta + 2\alpha^2\theta^2 + \cdots \quad ,$$

where the coefficient α determines the nonspecular or umklapp reflection probability for finite angle of incidence θ (again measured between the incident velocity and the surface plane). Second, the coefficient α is largest for electrons at points where the Fermi-surface radius of curvature is largest (e.g., for belly electrons in the case of Cu).

Both these qualitative statements are true for electron scattering from surface roughness, unfortunately.[4,5] In fact, the nonspecularity coefficient α for surface roughness scattering depends more strongly upon the Fermi-surface radius of curvature than it does for umklapp surface scattering. Thus, unless the surface roughness scattering is reduced to very small values by special surface preparation, it seems most appropriate to search for the umklapp scattering at necks or pocket regions of high curvature.

The umklapp mechanism does have a strong anisotropy with respect to the *plane* of incidence, and by comparing experiments done on different samples one may attempt to identify the umklapp surface scattering via this anisotropy. The other possibility for a clear identification of the umklapp scattering comes from the singularities in $P(\theta)$ at finite angles θ_0, which will be studied in this section.

The probability $P(\theta)$ of specular reflection discussed here is the diagonal probability $P_{11}(\theta)$ of Sec. II. The jump-scattering events should not be referred to as diffuse scattering, however, because for smooth surfaces the jump scattering is confined to a definite direction in space (see Fig. 3).

The small-angle expansion of $P_{ij}(\theta)$ is obtained by expanding R_{ij} in powers of the angle θ, assuming $R_{ij}(\theta)$ to be *analytic* for small angles. The assumption of analyticity is a strong assumption but

is not unreasonable. It is borne out by the model calculations of Sec. IV and also by the very nature of Eqs. (12). For example, $R_{11}(\theta)$ obeys Eq. (12a),

$$R_{11}(-\theta) = 1/R_{11}(\theta) \quad ,$$

and this equation is not compatible with a pole or other simple singularity at $\theta = 0$. Thus it is reasonable to assume that R_{ij} is analytic about $\theta = 0$.

A first and most obvious consequence of Eq. (12a) is that $R_{11}(0)$ must be (plus or minus) unity. For electrons inside a containing surface, the negative sign is correct, and the expansion then is

$$R_{11}(\theta) = -1 + a_1\theta + a_2\theta^2 + \cdots \quad . \tag{15}$$

The second coefficient in this expansion is determined in terms of a_1 by Eq. (12a);

$$a_2 = -\tfrac{1}{2}a_1^2 \quad . \tag{15'}$$

Setting $a_1 = \alpha + i\beta$, we conclude that

$$P_{11}(\theta) = |R_{11}|^2 = 1 - 2\alpha\theta + 2\alpha^2\theta^2 + \cdots \quad . \tag{16}$$

The coefficient of θ^2 in Eq. (16) is determined in terms of the coefficient of θ, and this is a very general characteristic of surface scattering which also holds for scattering from fine-scale surface roughness or from adsorbed atomic impurities. The relation is weakened to an inequality for a surface with large-scale surface roughness.[5,6]

The reflection amplitude $R_{12}(\theta)$ obeys Eq. (12b),

$$R_{12}(-\theta) = R_{12}(\theta)/R_{11}(\theta) \quad ,$$

and in view of Eq. (15) this implies that R_{12} is proportional to θ for small angles. If it is assumed that

$$R_{12}(\theta) = b_1\theta + b_2\theta^2 + \cdots \quad , \tag{17}$$

then substitution into Eq. (12b) yields

$$b_2 = -\tfrac{1}{2}a_1 b_1 \quad . \tag{17'}$$

A connection between b_1 and a_1 is also readily established via Eq. (6a). Because of the assumed symmetry of the crystal, one expects that

$$v_i = v_i^0 + O(\theta^2), \quad i = 1, 2 \tag{18}$$

$$\phi = \phi^0 + O(\theta^2) \quad , \tag{18'}$$

where the superscript 0 denotes the extremal values. Then inserting Eqs. (16) and (17) into Eq. (6a), one finds

$$|b_1|^2 = 2\alpha v_1^0/v_2^0(\sin\phi)^0 \quad . \tag{19}$$

The phase angle χ associated with b_1,

$$b_1 = |b_1| e^{i\chi} \quad , \tag{19'}$$

is not determined.

The next reflection amplitude is $R_{21}(\theta)$, which obeys Eq. (12c),

$$R_{21}(-\theta) = -\frac{R_{21}(\theta)}{R_{11}(\theta)} \quad .$$

This equation is compatible with a nonzero value for zero angle,

$$R_{21}(\theta) = c_0 + c_1\theta + \cdots \quad . \tag{20a}$$

Substitution into Eq. (12c) yields

$$c_1 = -\tfrac{1}{2}a_1 c_0 \quad , \tag{20b}$$

and then substitution into Eq. (8) gives

$$c_0 = b_1 \frac{v_2^0(\sin\phi)^0}{v_1^0} \tag{20c}$$

The final reflection amplitude is $R_{22}(\theta)$. The appropriate expansion is

$$R_{22}(\theta) = d_0 + d_1\theta + \cdots \quad . \tag{21a}$$

Substitution into Eq. (12d) yields

$$d_1 = -\tfrac{1}{2}b_1 c_0 \quad , \tag{21b}$$

but it is also clear that $|d_0|^2 = 1$ because $P_{22}(\theta)$ must approach unity for small angles θ where $P_{21} = P_{12}$ will vanish. Even the value of this unimodular number d_0 is determined in terms of the phase angle χ of Eq. (19') as

$$d_0 = e^{2i\chi} \quad , \tag{21c}$$

which is verified by substitution of (20) and (21) into Eq. (6b).

All the quantities appearing in the small-angle expansion are thus parametrized in terms of $a_1 = \alpha + i\beta$ and χ. It may readily be verified that the parametrized amplitudes obey the remaining equations such as Eq. (6c). However, this parametrization does not itself give us any idea of the numerical magnitude of the parameter α.

The value of α, and hence the importance of the umklapp scattering, can be calculated only by making a more detailed model of the surface physics (surface potentials, boundary conditions, and "band-bending" phenomena). On the other hand, it is possible to give an argument to show that the relative value of α is largest where the radius of curvature of the Fermi surface is largest.

Although the argument given here is based on the idealized Fermi-surface model of Fig. 2, it seems plausible that the qualitative result is generally valid. The key feature of this Fermi-surface model is the close proximity of the value of $\vec{K}_{\parallel}$ for which $\theta = 0$ to that for which $\phi = 0$. Because of this proximity it is possible to make a simultaneous expansion for small values of both θ and ϕ, and with this expansion one can compare the grazing-incidence behavior on the two sheets of the Fermi surface.

If the "belly" electrons (of type ϕ_1) are at grazing incidence, the angle θ is small and the specular

reflection probability is

$$P_{11} = 1 - 2\alpha\theta + 2\alpha^2\theta^2 + \cdots \quad ,$$

as was shown above. The umklapp scattering probability is

$$P_{12} = 2\alpha\theta - 2\alpha^2\theta^2 + \cdots \quad . \tag{22}$$

A similar expansion is appropriate about the other extremal point, where the "neck" electrons (of type ϕ_2) are at grazing incidence and the angle ϕ is small. This expansion is

$$P_{22} = 1 - 2\alpha'\phi + 2\alpha'^2\phi^2 + \cdots \quad ,$$

which defines the expansion coefficient α' associated with the extremal point for the neck electrons. In the vicinity of this latter extremal point the umklapp scattering probability is

$$P_{21} = P_{12} = 2\alpha'\phi - 2\alpha'^2\phi^2 + \cdots \quad . \tag{22'}$$

If the two segments of the Fermi-surface overlap only a little, and the projected extremal points are close together, then one may attempt a simultaneous expansion over the region where both θ and ϕ are small. This expansion has the form

$$P_{12} = 2\gamma\theta\phi - 2\gamma^2\theta^2\phi^2 + \cdots \quad , \tag{23}$$

where γ is a new coefficient. Equation (23) is compatible with (22) and (22') if

$$\alpha = \gamma\phi_0 \, , \quad \alpha' = \gamma\theta_0 \quad ,$$

where θ_0 is the value of θ for which ϕ is zero, and ϕ_0 is the value of ϕ for which θ is zero [e.g., recall Eq. (18')]. If the Fermi surfaces are locally spherical, it follows from the geometry that

$$K_1\theta_0^2 \cong K_2\phi_0^2 \quad ,$$

where K_1 and K_2 are the corresponding radii of curvature. Thus

$$\alpha/\alpha' \cong (K_1/K_2)^{1/2} \tag{24}$$

and so α is larger than α' if $K_1 > K_2$ (as in Fig. 2). In this sense the jump scattering is more important for electrons at points where the Fermi-surface radius of curvature is largest.

It seems important to qualify this observation by recalling that the surface roughness scattering is even more strongly dependent on the local radius of curvature of the Fermi surface, according to existing theories of surface roughness scattering.[5] Thus an experimental search for umklapp surface scattering is more likely to succeed at a point of small radius of curvature (neck or pocket states) where the roughness scattering is weaker.

The argument leading to Eq. (24) is very specialized, but the result is probably more generally true. The factors θ and ϕ which led to Eq. (24) have their origin in the constrained density of states

$$\int \delta(E_F - E_k)\, \delta(\vec{k}_{\parallel} - \vec{K}_{\parallel})\, d^3k \propto \frac{1}{\hat{n} \cdot \vec{v}_k} \quad ,$$

which enters reflection probabilities as in Eq. (4'). It is very plausible to suggest that these state-density factors dominate the angle dependence of the reflection probabilities in general.

The picture of surface reflection behavior may be extended further by examination of Eq. (23). For values of ϕ less than the critical value ϕ_0, θ is related to ϕ by

$$\theta = \left(\frac{K_2}{K_1}(\phi_0^2 - \phi^2)\right)^{1/2} = \phi_0\left(\frac{K_2}{K_1}\right)^{1/2}\left[1 - \left(\frac{\phi}{\phi_0}\right)^2\right]^{1/2} \tag{25}$$

for the spherical geometry of Fig. 2. Inserting this value into Eq. (23) we obtain the approximation

$$P_{12} = 2\alpha'\phi[1 - (\phi/\phi_0)^2]^{1/2} - 2\alpha'^2\phi^2[1 - (\phi/\phi_0)^2] + \cdots \tag{23'}$$

for the angle dependence of P_{12} in the range $0 < \phi < \phi_0$.

According to Eq. (23'), the umklapp scattering vanishes linearly with angle as ϕ approaches zero, but it vanishes with a more dramatic *square-root* dependence as ϕ approaches ϕ_0. There is no jump scattering for $\phi > \phi_0$ for the Fermi-surface geometry of Fig. 2.

At and near the angle ϕ_0, electrons on the "neck" portion of the Fermi surface are coupled, by the crystal surface, to the extremal states of the "belly" part of the Fermi surface. This coupling appears as a square-root dependence of the specular reflection probability; this singularity is a threshhold singularity.

Observation of such square-root singularities would make possible an experimental comparison of the relative location of two extremal points on the Fermi surface.

The singularity predicted for the Fermi surface of Fig. 2 is a sharp narrowing of the surface-state-resonance (SSR) linewidth (for electrons of type ϕ_2) when the angle of incidence exceeds ϕ_0 and the jump scattering becomes impossible. In this case the grazing-incidence electrons with angles $\phi < \phi_0$ would be, generally speaking, *more strongly* (non-specularly) scattered than electrons of larger angles of incidence. While strictly in agreement with Eq. (16), this behavior contradicts the spirit of the trend toward specular reflection at grazing incidence deduced from theories of surface roughness or contamination scattering.[4-7]

If the Fermi-surface geometry is slightly different, one may find the opposite sort of singularity, in which the jump scattering suddely becomes pos-

sible at a critical angle of incidence. In this case, the probability of specular reflection would be unity up to the critical angle, and then decrease abruptly via a square-root law. In this case, the SSR linewidth would not obey the H, $H^{4/3}$, or H^2 laws discussed in the literature.[5]

IV. SURFACE BOUNDARY CONDITION

In this section the surface reflection coefficients are approximately expressed in terms of matrix elements of the Bloch functions and a surface boundary condition. We do not attempt to obtain numerical values for R_{ik} but rather aim to verify and clarify the results obtained above from symmetry considerations. This is done by showing that a natural sequence of approximations yields a reflection matrix which obeys Eq. (12). The result also demonstrates that the umklapp process does not occur if the surface boundary condition is $\Psi = 0$ on the surface plane.

Expressions will be sought for the reflection coefficients R_{ik} in the scattering state

$$\Psi_1(\vec{r}) = \phi_1(\vec{r}) + R_{11}\tilde{\phi}_1(\vec{r}) + R_{12}\tilde{\phi}_2(\vec{r}) \quad . \tag{2}$$

As mentioned in Sec. II, the true scattering eigenfunction contains a term localized near the metal surface, which was denoted $\Psi_1^{\rm loc}(\vec{r})$ in Eq. (1). This localized term contains "band-bending" effects associated with the electrostatic potential of the metal surface, as well as alterations in the Bloch functions associated with lattice relaxation in the surface layers.

During the symmetry discussion of Sec. II, the wave function was examined in the asymptotic region (far from the surface) where it was quite proper to neglect the surface term $\Psi_1^{\rm loc}$. However, in the present discussion, Eq. (2) is used even near the nominal surface plane, and $\Psi_1^{\rm loc}$ will be neglected as an *approximation*. It would seem that this approximation is reasonable in metals, if not in semiconductors.

We consider a crystal which has inversion symmetry with respect to some point in the unit cell, and choose that point as the origin of coordinates. The coordinate axes are aligned along appropriate crystal axes, and the crystal surface is normal to the $\hat{z}$ direction ($z > 0$ is the region outside the crystal). It is also assumed that the (infinite) crystal would have reflection symmetry in the plane $z = 0$.

The plane $z = 0$ defines the "surface" in the following sense: it is assumed that all atoms entirely in the region $z > 0$ are removed, and the remaining atoms held rigidly in their original positions (omitting lattice relaxation effects). The last layer of atoms (near the plane $z = 0$) will give electrostatic equipotential surfaces which extend into the region $z > 0$, but the effects of this potential (and the work-function barrier) are described by a boundary-condition function $D(x, y)$, which is the logarithmic derivative of an eigenfunction on the plane $z = 0$:

$$\Psi_j(x, y, 0)\, D(x, y) = \frac{\partial}{\partial z}\Psi_j(x, y, 0) \quad . \tag{26}$$

This eigenfunction, and hence $D(x, y)$, depends upon the energy E and the conserved parallel wave vector $\vec{K}_{\parallel}$. $D(x, y)$ is periodic in the surface plane, with periods induced by the lattice symmetry. $D(x, y)$ could also be determined by seeking the solution of the Schrödinger equation in the region $z > 0$ which has the specified energy $E = E_F$, appropriate wave vector parallel to the surface plane, and approaches zero as $z \to \infty$. Since this solution is unique, the same boundary-condition function $D(x, y)$ applies to both Ψ_1 and Ψ_2.

It is useful to define special matrix elements

$$\begin{aligned} D_{ij} &\equiv \int \phi_i^*(x, y, 0)\, D(x, y)\, \phi_j(x, y, 0)\, dx\, dy \quad , \\ Q_{ij} &\equiv \int \phi_i^*(x, y, 0) \frac{\partial}{\partial z}\phi_j(x, y, 0)\, dx\, dy \quad , \end{aligned} \tag{27}$$

where the two-dimensional integrals are taken over a unit cell in the surface plane. The values of the matrix elements are the same for any surface cell, since all the Bloch functions under consideration have the same fixed parallel wave vector $\vec{K}_{\parallel}$. We shall use the notation $D_{i\bar{k}}$ for the matrix element involving $\tilde{\phi}_k$:

$$D_{i\bar{k}} \equiv \int \phi_i^*(x, y, 0)\, D(x, y)\, \tilde{\phi}_k(x, y, 0)\, dx\, dy \quad .$$

In terms of these matrix elements, Eq. (26) becomes

$$\begin{aligned} D_{11} + R_{11} D_{1\bar{1}} + R_{12} D_{1\bar{2}} &= Q_{11} + R_{11} Q_{1\bar{1}} + R_{12} Q_{1\bar{2}} \quad , \\ D_{21} + R_{11} D_{2\bar{1}} + R_{12} D_{2\bar{2}} &= Q_{21} + R_{11} Q_{2\bar{1}} + R_{12} Q_{2\bar{2}} \quad . \end{aligned} \tag{28}$$

Equations (28) are obtained by multiplying (26) by $\phi_i^*(i = 1, 2)$ and integrating over the unit surface cell.

Under the conditions described there is a close connection between the Bloch functions ϕ_k and $\tilde{\phi}_k$, which follows from the assumed reflection symmetry of the original (infinite) crystal. As a consequence of this symmetry,

$$\tilde{\phi}_k(\vec{r}) = A_0\, \phi_k(\vec{\bar{r}})$$

where $\vec{\bar{r}}$ is the image point associated with r:

$$\vec{r} = (x, y, z), \quad \vec{\bar{r}} = (x, y, -z) \quad ,$$

and where A_0 is a possible phase factor which will be neglected for convenience (the analysis is easily generalized to include A_0). It follows that

$$\begin{aligned} &\tilde{\phi}_k(x, y, 0) = \phi_k(x, y, 0) \quad , \\ &\left(\frac{\partial \tilde{\phi}_k}{\partial z}\right)_{z=0} = -\left(\frac{\partial \phi_k}{\partial z}\right)_{z=0} \quad , \end{aligned} \tag{29}$$

which implies the relations

$$D_{i\bar{j}} = D_{ij} \ , \quad Q_{i\bar{j}} = -Q_{ij} \quad . \tag{29'}$$

With these relations, it is easy to solve Eqs. (28) to obtain the reflection coefficients

$$R_{11} = -\frac{(D_{11}-Q_{11})(D_{22}+Q_{22}) - (D_{12}+Q_{12})(D_{21}-Q_{21})}{(D_{11}+Q_{11})(D_{22}+Q_{22}) - (D_{12}+Q_{12})(D_{21}+Q_{21})} \ , \tag{30}$$

$$R_{12} = \frac{(D_{11}-Q_{11})(D_{21}+Q_{21}) - (D_{21}-Q_{21})(D_{11}+Q_{11})}{(D_{11}+Q_{11})(D_{22}+Q_{22}) - (D_{12}+Q_{12})(D_{21}+Q_{21})} \ . \tag{31}$$

With these formulas we may examine the case of the special boundary condition $\Psi = 0$ for $z = 0$. This boundary condition, although physically unrealistic, has often been used in studies of surface reflection or surface physics.[5,14,16] In this case, it has the effect of altogether removing the phenomena of interest.

If $D(x, y)$ approaches the infinity uniformly, the boundary condition of Eq. (26) becomes

$$\Psi_j(x, y, 0) = 0 \quad .$$

In that case, the matrix element D_{ij} becomes much larger than Q_{ij} in Eqs. (30) and (31) and the limiting behavior is

$$\lim_{D\to\infty} R_{11} = -1 \ , \quad \lim_{D\to\infty} R_{12} = 0 \tag{32}$$

(assuming that $D_{11}D_{22} - D_{12}D_{21}$ does not accidentally vanish). Thus there is no umklapp surface scattering for this boundary condition. The boundary condition $\Psi = 0$ is too extreme because the work function is not infinite.

It is also possible to verify the negative-angle symmetry from Eqs. (30) and (31). This is seen by replacing 1 by $\bar{1}$ in the right-hand subscripts throughout Eqs. (30) and (31), which is the analytic continuation of R_{ij} to negative angles of incidence for ϕ_1. In the case of Eq. (30), for example, this gives

$$\begin{aligned} R_{1\bar{1}} &= R_{11}(-\theta) \\ &= -\frac{(D_{1\bar{1}}-Q_{1\bar{1}})(D_{22}+Q_{22}) - (D_{12}+Q_{12})(D_{2\bar{1}}-Q_{2\bar{1}})}{(D_{1\bar{1}}+Q_{1\bar{1}})(D_{22}+Q_{22}) - (D_{12}+Q_{12})(D_{2\bar{1}}+Q_{2\bar{1}})} \\ &= -\frac{(D_{11}+Q_{11})(D_{22}+Q_{22}) - (D_{12}+Q_{12})(D_{21}+Q_{21})}{(D_{11}-Q_{11})(D_{22}+Q_{22}) - (D_{12}+Q_{12})(D_{21}-Q_{21})} \\ &= \frac{1}{R_{11}(\theta)} \ , \end{aligned}$$

which agrees with Eq. (12a). It is easily verified that Eq. (31) obeys the symmetry of Eq. (12b) under the same transformation.

It should be noted that this symmetry property holds for any values of D_{ij}, Q_{ij} that are compatible with Eqs. (29'). In fact the actual values of D_{ij}, Q_{ij} are not arbitrary or independent, but must be subjected to additional restrictions in order that Eq. (26) hold exactly true. These additional restrictions are also required in order that R_{ik} be compatible with Eqs. (6). However, the symmetry property (12) holds *a fortiori* in the presence of these additional restrictions.

The analysis given above makes various assumptions and approximations, and so it is not at all a discussion of the general case. However, the essential point is that a rather natural set of approximations leads to a reflection matrix which obeys the symmetry conditions Eq. (12) that are the basis of the discussion in Sec. III.

V. CONCLUSIONS

Umklapp surface scattering has been studied for a convenient special case in which the crystal surface is a low-index surface of a highly symmetric crystal. The original bulk crystal is assumed to have reflection symmetry with respect to planes equivalent to the surface plane, and also 180° rotation symmetry about the surface normal. These restrictions greatly simplify the analysis.

For the model Fermi surface of Fig. 2, there are two types of electron on the two sheets of the Fermi surface. The umklapp mechanism depends on the existence of such inequivalent points, having the same component of wave vector parallel to the crystal surface. Such points exist for almost all multivalent metals and even for Cu, Ag, and Au at certain Fermi-surface positions.

The umklapp scattering probability varies *linearly* with angles of incidence and the scattering becomes specular at grazing incidence [Eq. (16)]:

$$P(\theta) = 1 - 2\alpha\theta + 2\alpha^2\theta^2 + \cdots \quad .$$

The coefficient $2\alpha^2$ of the quadratic term is determined in terms of the coefficient 2α of the linear term, in this small-angle expansion. The value of α depends on the Fermi-surface position of the electrons under consideration, and may be different for grazing-incidence electrons at different regions or sheets of the Fermi surface.

A comparison of two small-angle expansions showed that

$$\alpha_j \propto \sqrt{K_j} \quad ,$$

where K_j is the radius of curvature of the Fermi surface near point j. This result is quite plausible, but the argument presented for it was not very general or rigorous.

If the result is generally true, the umklapp mechanism most strongly affects electrons on large pieces of the Fermi surface where the radius of curvature is large. However, it should be strongly emphasized that other surface scattering

mechanisms (e.g., surface roughness scattering[4,5]) depend even more strongly on K_j. Thus electrons of small pockets or necks probably offer a better opportunity to observe the umklapp scattering in competition with unavoidable surface roughness.

For certain values of the angle of incidence θ, the parallel component of the wave vector reaches an extremal point on another sheet of the Fermi surface. In this case, on one side of the critical angle θ_0 the jump scattering is possible, while it is not possible on the other side. This situation leads to a characteristic threshhold singularity in the angle dependence of the probability of specular reflection.

By utilization of the reciprocity relation $P_{12}=P_{21}$ of Eq. (9) above, and the grazing-incidence expansion for electrons on the distant sheet, one can readily show that near the singularity the reflection coefficient has a square-root angle dependence. The probability of specular reflection has the approximate form

$$P(\theta)\cong\begin{cases}1, & \theta>\theta_0\\ 1-A[1-(\theta/\theta_0)^2]^{1/2}, & \theta<\theta_0\end{cases}$$

near the critical angle θ_0, assuming the jump scattering can occur only for $\theta<\theta_0$.

The calculations of Sec. IV showed that a natural sequence of approximations leads to a reflection matrix compatible with the negative-angle symmetry of Sec. II. It was also shown that the umklapp surface scattering does not arise for the unrealistic, but commonly used, boundary condition that the electron wave function vanish at the crystal surface.

Surface-state-resonance experiments are most suitable for an attempt to directly observe and isolate the umklapp surface scattering. There are two evident ways to identify umklapp scattering: one approach is to exploit the anistropy of the umklapp scattering with respect to the plane of incidence of the electrons, while the other approach is to attempt to observe the critical-angle singularities for a material in which these singularities occur near grazing incidence.

The umklapp surface scattering mechanism may also play an interesting role in several other physical phenomena. In the high-frequency regime (Holstein limit) of the anomalous skin effect, the absorption of electromagnetic radiation by a metal is determined in large part by the nature of electron surface reflection. Nonspecular reflection of electrons is associated with absorption of the infrared radiation. There is the possibility that umklapp surface scattering sets the limitation, in principle, on the quality of metallic mirrors in the infrared-radiation regime. This possibility appears to have some contemporary technological interest.

Another problem involving the umklapp surface reflection is quantum-limit behavior in thin films. If the films are sufficiently thin, pure, and smooth that size quantization may occur the surface mixing of standing waves (via the umklapp process) will give rise to several interesting phenomena requiring careful investigation.

ACKNOWLEDGMENTS

We wish to acknowledge useful and helpful discussions with M. P. Garfunkel, D. Lessie, and W. J. Choyke.

APPENDIX

This appendix will indicate how the definition of reflection probability, Eq. (4) of Sec. II, follows naturally from a wave-packet description of the surface scattering.

We imagine a large incident wave train in the form of a rectangular packet of cross-section area A_1 and thickness (along the direction of motion) l_1. This wave packet, associated with state ϕ_1, has the angle of incidence θ. It is assumed that all dimensions of the wave packet are enormously larger than the electron wavelength, so that one may completely neglect wave-packet distortion during the motion. In fact, if the wave packet is sufficiently large, the central region of the wave packet is dominant, and this central region is assumed to be be essentially the pure Bloch state ϕ_1. The precise form of the edges of the wave packet does not matter if the packet is sufficiently large.

If the Bloch function ϕ_j is normalized to unity on the unit cell, as in Eq. (3′), then the total incident probability is

$$P_{\text{inc}}=A_1 l_1/\Omega_0 \quad ,$$

where Ω_0 is the volume of the unit cell.

When this wave packet strikes the crystal surface, it covers a surface area (in the surface plane)

$$A=A_1/\sin\theta \quad ,$$

where θ is again measured between the incident velocity and the surface plane. The duration of the collision is a time $\tau=l_1/v_1$, where v_1 is the magnitude of the velocity.

Two reflected wave packets will emerge from the crystal surface after the collision, one of type $\bar{\phi}_1$ and the other of type $\bar{\phi}_2$. The reflected wave of type $\bar{\phi}_1$ will have the same geometrical configuration as the incident wave packet (i.e., the same cross-sectional area A_1 and the same longitudinal length l_1) but the total probability carried is less because the amplitude of the reflected wave $\bar{\phi}_1$ is reduced by the factor R_{11}. The reflected probab-

ability in the specularly reflected packet $\tilde{\phi}_1$ is thus

$$P_{(1)} = A_1 l_1 |R_{11}|^2/\Omega_0 \quad ,$$

which is some fraction of the probability incident.

The second wave packet has slightly different geometrical properties. Its area A_2 and thickness l_2 are generated by the collision area A and collision duration τ according to

$$A_2 = A \sin\phi \, , \quad l_2 = v_2 \tau \quad ,$$

so the reflected probability in this second wave packet is

$$P_{(2)} = A_2 l_2 |R_{12}|^2/\Omega_0 \quad .$$

The statement of probability conservation now reads

$$A_1 l_1 |R_{11}|^2 + A_2 l_2 |R_{12}|^2 = A_1 l_1 \quad ,$$

which is easily transformed into the form given in Eq. (6a),

$$|R_{11}|^2 + \frac{v_2 \sin\phi}{v_1 \sin\theta} |R_{12}|^2 = 1$$

The geometrical factors encountered in this discussion have been mentioned by various authors under names such as "aspect effect" or "collision duration effect."[2,12] Velocity factors, of similar origin, are well known in nuclear-reaction scattering theory.

The definition of reflection probability adopted here leads to the detailed balance principle in the form of Eq. (9). A quite-different form of this principle (with velocity factors for initial and final states) is encountered in discussions of diffuse surface scattering.[15,20] However, in the case of diffuse scattering one deals with a *differential* scattering cross section, which has different definition according to the choice of volume element. It is not difficult to formulate diffuse scattering theory in such a way that the detailed balance principle appears in the form of Eq. (9) with the proper choice of volume element for the diffuse reflection probability.

---

*Research supported by the Air Force Office of Scientific Research, Office of Aerospace Research, USAF, under Grant No. AFOSR 71-2028 A.

[1]The magnetic surface-state-resonance experiments are reviewed by J. F. Koch [in *Simon Fraser University Lectures: Solid State Physics*, edited by J. Cochran and R. Haering (Gordon and Breach, New York, 1968), Vol. I] and by M. S. Khaikin {Usp. Fiz. Nauk 96, 409 (1969) [Sov. Phys.-Usp. 11, 785 (1969)]}.

[2]R. E. Doezema and J. F. Koch, Phys. Rev. B 5, 3866 (1972); Phys. Rev. B 6, 2071 (1972); J. F. Koch and T. E. Murray, Phys. Rev. 186, 722 (1969); R. Doezema, J. F. Koch, and U. Strom, Phys. Rev. 182, 717 (1969); T. W. Nee, J. F. Koch, and R. E. Prange, Phys. Rev. 174, 758 (1968); R. E. Prange and T. W. Nee, Phys. Rev. 168, 179 (1968).

[3]T. Kennedy and G. Seidel, Phys. Rev. B 6, 3706 (1972); J. P. Rahn and J. J. Sabo, Phys. Rev. B 6, 3666 (1972); R. Goodrich *et al.*, Phys. Rev. B 5, 1202 (1972).

[4]Experimental observation of the effects of surface roughening is reported by J. F. Koch and T. E. Murray, Phys. Rev. 186, 722 (1969).

[5]H. J. Fischbeck and J. Mertsching, Phys. Status Solidi 27, 345 (1968); Phys. Status Solidi 41, 45 (1970); L. Fal'kovskii, Zh. Eksp. Teor. Fiz. 58, 1830 (1970), [Sov. Phys.-JETP 31, 981 (1970)]; Zh. Eksp. Teor. Fiz. 60, 838 (1971) [Sov. Phys.-JETP 33, 454 (1971)]; E. Kaner, N. Makarov, and I. Fuks, Zh. Eksp. Teor. Fiz. 55, 931 (1968) [Sov. Phys.-JETP 28, 483 (1969)].

[6]R. More and D. Lessie, Phys. Rev. B 8, 2527 (1973).

[7]M. Watanabe, Surf. Sci. 34, 759 (1973); J. W. Geus, in *Chemisorption and Reactions on Metallic Films*, edited by J. Anderson (Academic, London, 1971), Vol. I.

[8]The surface reflection process considered in this paper is one in which the component of wave vector parallel to the surface is conserved (in the reduced zone scheme) and the normal component changes. For the special case of a polyvalent metal with a nearly-free-electron Fermi surface, this process appears in the extended zone scheme as an umklapp transition at the surface. That is the only sense in which the word umklapp is properly used for the transitions considered here. The term intervalley surface scattering is used to describe the same process in semiconductors.

[9]P. J. Price, I.B.M. J. Res. Dev. 4, 152 (1960).

[10]A. B. Pippard, *Dynamics of Conduction Electrons*. (Gordon and Breach, New York, 1965), p. 46.

[11]R. Chambers, in *The Physics of Metals*, edited by J. Ziman (Cambridge U. P., Cambridge, 1969), Vol. I, p. 183.

[12]R. F. Greene, in *Solid State Surface Science, Vol. I*, edited by M. Green (Marcel Dekker, New York, 1969)

[13]A. N. Friedman, Phys. Rev. 159, 553 (1967).

[14]F. Stern and W. Howard, Phys. Rev. 163, 816 (1967).

[15]V. Kravchenko and E. Rashba, Zh. Eksp. Teor. Fiz. 66, 1713 (1969) [Sov. Phys.-JETP 29, 918 (1969)].

[16]A. Andreev, Usp. Fiz. Nauk 105, 113 (1971) [Sov. Phys. Uspekhi 14, 609 (1972).

[17]In this paper we consider a restricted case for which the Fermi surface has reflection symmetry with respect to the crystal surface plane and also 180° rotation symmetry about the surface normal, rather than the more general situation suggested by the drawings in papers of Price (Ref. 9) or Pippard (Ref. 10). It is our belief that the cases considered by those authors would involve a surface without the complete translational symmetry of the bulk, and hence a breakdown of the conservation law for $\vec{K}_{\parallel}$.

[18]It is obvious, physically, that any scattering state is uniquely specified by its incident part. A formal proof might be constructed on the basis of the time-dependent

collision theory as presented, for example, by J. R. Taylor, in *Scattering Theory* (Wiley, New York, 1972).

[19]J. Blatt and V. Weiskopf, *Theoretical Nuclear Physics* (Wiley, New York, 1952).

[20]Strictly speaking, Eq. (9) does not correspond to the usual principle of detailed balance because the pairs of transitions involved are not between identical states. This point is discussed by F. Garcia-Moliner and S. Simons [Proc. Camb. Phil. Soc. 53, 848 (1957)]. Often statements of the detailed balance principle for surface collisions are made in which factors of the perpendicular velocity component appear. These statements are correct, but refer to the case of diffuse scattering. For diffuse scattering, the final states form a continuum, and a volume element must be specified to unambiguously define a reflection probability. If the volume element is d^3k, as in the work of Moliner-Simons, one has the velocity factors; if the volume element is $dE\, d^2\vec{K}_{\parallel}$, the resulting reflection probability obeys detailed balance in a form like Eq. (9).

[21]J. R. Taylor, in Ref. 18.